

Direct observation of mixing of spin-multiplets in an antiferromagnetic molecular nanomagnet by electron paramagnetic resonance

S. Datta,¹ O. Waldmann,² A. D. Kent,³ V. A. Milway,⁴ L. K. Thompson,⁴ and S. Hill¹

¹*Department of Physics, University of Florida, Gainesville, Florida 32611, USA*

²*Department of Chemistry and Biochemistry, University of Bern, CH-3012 Bern, Switzerland*

³*Department of Physics, New York University, 4 Washington Place, New York, New York 10003, USA*

⁴*Department of Chemistry, Memorial University, St. Johns, Newfoundland, Canada A1B 3X7*

(Dated: November 20, 2018)

High-frequency electron paramagnetic resonance (EPR) studies of the antiferromagnetic Mn-[3×3] molecular grid clearly reveal a breaking of the $\Delta S = 0$ selection rule, providing direct evidence for the mixing of spin wavefunctions (S -mixing) induced by the comparable exchange and magneto-anisotropy energy scales within the grid. This finding highlights the potential utility of EPR for studies of exchange splittings in molecular nanomagnets, which is normally considered the sole domain of inelastic neutron scattering, thereby offering improved sensitivity and energy resolution.

PACS numbers: 33.15.Kr, 71.70.-d, 75.10.Jm

The synthesis of ordered crystalline arrays (ensembles) of nominally identical magnetic molecules has enabled unprecedented insights into quantum magnetization dynamics at the nanoscale, leading to exciting discoveries such as the quantum interference associated with the coherent rotation (tunneling) of a large spin [1]. The molecular approach is particularly attractive due to the highly ordered and monodisperse nature of the molecules in the solid state, and because one can systematically vary many key parameters that influence the quantum behavior of a magnetic molecule, e.g., the total spin, symmetry, etc. The magnetism of these molecules can be described quite generally by the microscopic spin Hamiltonian [2]

$$\hat{H} = - \sum_{ij} J_{ij} \hat{\mathbf{s}}_i \cdot \hat{\mathbf{s}}_j + \sum_i \hat{\mathbf{s}}_i \cdot \mathbf{D}_i \cdot \hat{\mathbf{s}}_i + g\mu_B \hat{\mathbf{S}} \cdot \mathbf{B}. \quad (1)$$

The first term parameterizes the Heisenberg interaction between each pair of magnetic ions; $\hat{\mathbf{s}}_i$ are the spin operators at each site, and J_{ij} the respective coupling constants. The second term accounts for the magnetic anisotropy at each site; \mathbf{D}_i are the local zero-field-splitting (ZFS) tensors. The final term is the Zeeman interaction written in terms of the total spin operator $\hat{\mathbf{S}}$.

In the strong exchange limit, the total spin S is a good quantum number and the exchange term splits the energy spectrum into well separated spin multiplets, each having comparatively weaker ZFS due to magnetic anisotropy [3]. However, as the ZFS increases relative to the exchange splitting, mixing of spin multiplets becomes significant (S -mixing) such that S no longer constitutes a good quantum number [4, 5]. This parameter regime has attracted growing interest due to the realization that S -mixing plays a crucial role in the quantum dynamics of coupled spin systems, namely in the tunneling terms in single-molecule magnets (SMMs) and antiferromagnetic (AF) clusters [6, 7, 8, 9], and in the novel magneto-oscillations associated with the total spin of a molecule [10, 11, 12]. Indeed, the interplay between anisotropy

and exchange is central to the understanding of (nano-) magnetism, and experimental determination of exchange and anisotropy splittings is of great value.

ZFS caused by magnetic anisotropy may be studied spectroscopically using both electron paramagnetic resonance (EPR) and inelastic neutron scattering (INS). In contrast, the most unambiguous method for estimating exchange couplings involves determining the exact locations of excited spin multiplets. For this reason, such investigations have been limited to INS, since the EPR selection rule $\Delta S = 0$ forbids excitations between spin multiplets (the INS selection rule $\Delta S = 0, \pm 1$ permit such *intermultiplet* transitions). In this work, we show that S -mixing indeed can give rise to a situation in which exchange splitting is observed directly in a nanomagnet using high-sensitivity multi-high-frequency EPR.

The Mn-[3 × 3] grid is an attractive candidate in the above context. Its structure consists of nine spin- $\frac{5}{2}$ Mn^{II} ions placed at the vertices of a 3 × 3 matrix, see Fig. 1(a). A significant magnetic anisotropy, demonstrated in previous experiments [13], gives rise to several striking effects, including novel quantum-oscillations in the field dependent magnetic torque [10], and tunneling of the Néel vector at high fields [14]. The magnetism of Mn-[3 × 3] can be well described by the approximate Hamiltonian

$$\begin{aligned} \hat{H}_1 = & -J_R \left(\sum_{i=1}^7 \hat{\mathbf{s}}_i \cdot \hat{\mathbf{s}}_{i+1} + \hat{\mathbf{s}}_8 \cdot \hat{\mathbf{s}}_1 \right) - J_C \sum_{j=1}^4 \hat{\mathbf{s}}_{2j} \cdot \hat{\mathbf{s}}_9 \\ & + D_R \sum_{i=1}^8 \hat{s}_{i,z}^2 + D_C \hat{s}_{9,z}^2 + g\mu_B \hat{\mathbf{S}} \cdot \mathbf{B}, \end{aligned} \quad (2)$$

with AF couplings $J \equiv J_R = J_C < 0$, and uniaxial easy-axis anisotropy $D \equiv D_R = D_C < 0$ (spins are numbered according to Fig. 1; z denotes the axis perpendicular to the grid) [10]. Here, we report the clear observation of an EPR transition between the $S = \frac{5}{2}$ ground state and the first excited $S = \frac{7}{2}$ spin multiplet, i.e., a $\Delta S = \pm 1$ transition.

The observation via EPR of *intermultiplet* transitions for a molecular nanomagnet is of significance from at least three points of view.

(1) It demonstrates that with today's EPR spectrometers it is possible to directly measure exchange splittings. This represents a significant development, with the potential to change the landscape of experiments on exchange coupled systems. EPR offers many advantages compared to INS, such as high-sensitivity (much smaller single crystals), "cheap" experimental environments, essentially unlimited spectral resolution permitting linewidth studies, etc..

(2) To date, the most direct evidence for S -mixing has involved measuring energy spacings in EPR and INS spectra, and then comparing these to calculations [8, 12]. In the present case, however, evidence comes from the observation of an otherwise forbidden EPR transition, i.e., breaking of the selection rule $\Delta S = 0$ – a property directly related to the wavefunctions. This is, hence, the most clear-cut experimental demonstration of S -mixing.

(3) $\text{Mn-[3} \times \text{3]}$ was the first molecule in which the effects of S -mixing were clearly demonstrated, and subsequent studies have shown that the generic Hamiltonian \hat{H}_1 provides a complete description of these effects [10]. The present EPR results confirm these findings and provide text-book quality insights into the physics of magnetic molecules and the effects of S -mixing.

Single crystals of $\text{Mn-[3} \times \text{3]}$, $[\text{Mn}_9(\text{2POAP-2H})_6(\text{ClO}_4)_6 \cdot 3.57\text{MeCN} \cdot \text{H}_2\text{O}]$, were prepared as reported [15]. They crystallize in the space group C_2/c . The cation $[\text{Mn}_9(\text{2POAP-2H})_6]^{6+}$ exhibits a slightly distorted S_4 molecular symmetry, with the C_2 axis perpendicular to the grid plane and parallel to the uniaxial magnetic easy (z -) axis. Single-crystal EPR spectra were obtained using a sensitive cavity perturbation technique. A vector network analyzer was used to record the complex signal (amplitude and phase) transmitted through the cavity; this technique is described in detail elsewhere [16]. Data were recorded for two samples. If not otherwise stated, the magnetic field was applied along the z axis.

Figure 1(a) displays the 62 GHz EPR spectrum obtained at 1.4 K. Five transitions labeled P_n ($n = 1, 2, 3, c, d$) are clearly observed. P_c is the $M = -\frac{1}{2} \rightarrow +\frac{1}{2}$ signal expected for a half-integer spin system, and will not be discussed in detail. The temperature dependence of the 52 GHz EPR spectrum is shown in Fig. 2. Upon increasing the temperature, additional transitions appear, e.g., P_4 , P_5 , and the rich fine structure around P_c , which is of no interest in this work. Above ~ 20 K, only a central line is observed, which is expected due to the thermal population of a large number of spin multiplets with negligible ZFS. In Fig. 1(b), we display the frequency dependence of the resonance fields B_n of the peaks P_n ($n = 1, \dots, 5, d$); each depends linearly on frequency due to the Zeeman term in Eq. (2). The ZFS may be obtained from the $B = 0$ intercepts by extrapolation. B_1

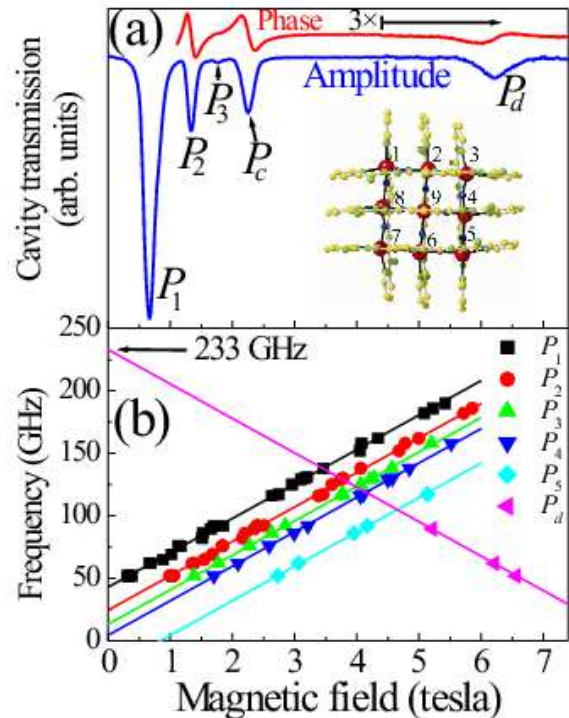


FIG. 1: (Color online) (a) Complex EPR spectrum at 1.4 K and 62 GHz. The dips in amplitude correspond to EPR; the sense of phase rotation through each dip differentiates $\Delta M = \pm 1$ transitions. The $\text{Mn-[3} \times \text{3]}$ grid is shown in the inset. (b) Frequency dependence of the resonance fields B_n of the indicated peaks; the solid lines represent best-fits (see text).

to B_5 increase with frequency; in contrast, B_d decreases with frequency as also seen from the sense of the phase rotation through the resonance [Fig. 1(a)]. A clear hint that P_d is not a usual intramultiplet transition ($\Delta S = 0$) is found from the large $B = 0$ offset of ~ 233 GHz. ZFS caused by magnetic anisotropy is much smaller for Mn^{II} complexes [17]. This suggests that the large offset for P_d is caused by exchange, i.e., P_d is an *intermultiplet* transition. Furthermore, previous magnetic and INS measurements determined the zero-field gap between the $S = \frac{5}{2}$ ground and first excited $S = \frac{7}{2}$ states to be 230 ± 10 GHz [10, 13], thus suggesting that P_d indeed corresponds to the $S = \frac{5}{2} \rightarrow \frac{7}{2}$ transition.

Before discussing P_d further, we focus on the analysis in terms of \hat{H}_1 , with the aim to obtain best-fit values for J and D . In a first step, we fit straight lines to the data in Fig. 1(b) with a common g factor, yielding values for the ZFS associated with each transition (see Table I) and $g = 1.970(7)$. We then determine J and D as follows. A least-squares fit based on the full Hamiltonian would be very demanding because its dimension is 10,077,696. However, it has previously been demonstrated that the energies and wavefunctions of the low-lying states of relevance

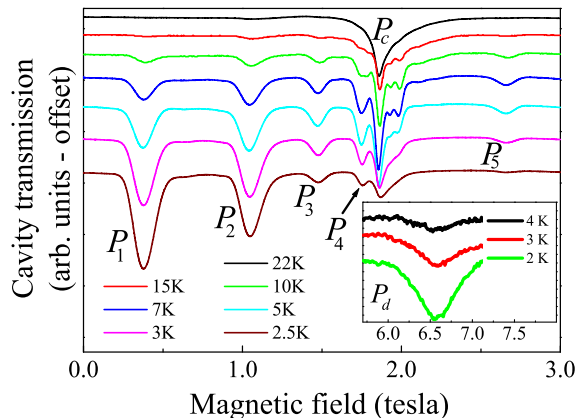


FIG. 2: (Color online) Temperature dependence of the EPR spectrum at 52 GHz; several of the transitions have been labeled. The inset shows the temperature dependence of transition P_d .

TABLE I: First line: Experimental ZFS determined from fits to the data in Fig. 1(b). Second line: Calculated ZFS using the best-fit J and D values. Energies are given in GHz.

P_1	P_2	P_3	P_4	P_5	P_d
42.7(3)	24.3(4)	13.2(5)	4.4(5)	-23.3(7)	233(1)
42.80	24.47	12.62	3.79	-24.47	233.0

here can be calculated with high accuracy from the effective spin Hamiltonian $\hat{H}_2 = -0.526J_R\hat{S}_A\cdot\hat{S}_B - J_C\hat{S}_A\cdot\hat{S}_9 + 0.197D_R(\hat{S}_{A,z}^2 + \hat{S}_{B,z}^2) + D_C\hat{S}_{9,z}^2 + g\mu_B\hat{S}\cdot\mathbf{B}$ [14]. A (B) denotes the sublattice of corner (edge) spins [see Fig. 1(a)], i.e., $\hat{S}_A = \hat{s}_1 + \hat{s}_3 + \hat{s}_5 + \hat{s}_7$ ($\hat{S}_B = \hat{s}_2 + \hat{s}_4 + \hat{s}_6 + \hat{s}_8$). The dimension of \hat{H}_2 is only 2646, permitting a true least-squares fit to the data. We obtain $J = -4.76(4)$ K and $D = -0.144(2)$ K, in very good agreement with previous experiments [10, 13]. The calculated ZFS values are compared to experiment in Table I; the agreement is excellent.

From a general point-of-view, our model for Mn-[3×3] appears over-simplified. Even if one assumes ideal symmetry, the exchange and anisotropy parameters need not be identical for all Mn^{II} ions in the Mn-[3×3] grid. Indeed, evidence for slight variations in the exchange constants was inferred from INS studies [13]. However, no variation was found from the present measurements, or from thermodynamic studies [10]. This is because the relevant energies are governed by the average of the exchange constants, hence only a single J is needed. Similar arguments apply to the anisotropy parameters and, in fact, no evidence for a variation has been reported so far. Consequently, the generic Hamiltonian \hat{H}_1 (or \hat{H}_2) with just the three parameters J , D , and g , captures all of the relevant physics and provides an excellent effective

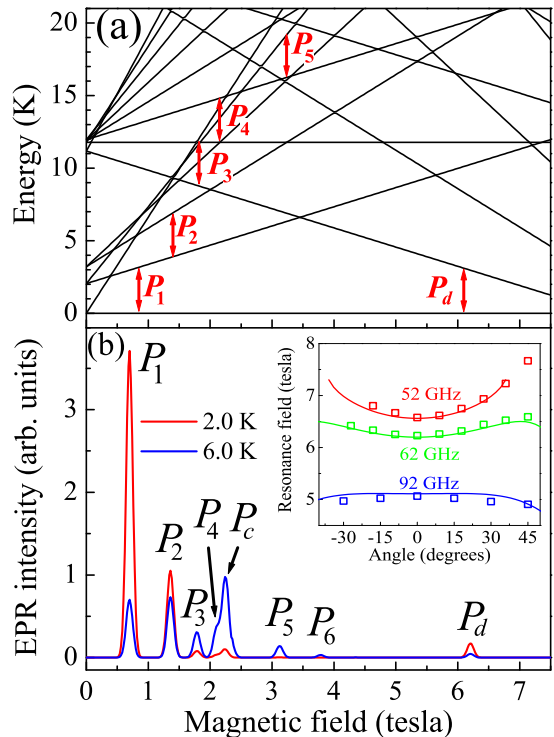


FIG. 3: (Color online) (a) Calculated energy spectrum (relative to the $S = \frac{5}{2}$, $M = -\frac{5}{2}$ ground state) for $B \parallel z$; several transitions are indicated. (b) Calculated EPR spectra at 62 GHz and two temperatures. The inset shows the angle dependence of B_d at three frequencies; experimental data are represented by open squares, and simulations by solid lines.

description of the low-energy properties of Mn-[3×3]. The EPR results presented here establish the most critical test so far.

The calculated low-energy, low-field spectrum for Mn-[3×3] is displayed in Fig. 3(a). It consists of a $S = \frac{5}{2}$ ground state and a first excited $S = \frac{7}{2}$ multiplet; these are further split into three and four $\pm M$ sublevels, respectively. In zero field, the $M = \pm\frac{5}{2}$ ($\pm\frac{7}{2}$) levels of the $S = \frac{5}{2}$ ($S = \frac{7}{2}$) multiplet lie lowest in energy due to the easy-axis anisotropy. The $\pm M$ sublevels split in magnetic field due to the Zeeman interaction. The $M = -\frac{5}{2} \rightarrow -\frac{3}{2}$, $M = -\frac{3}{2} \rightarrow -\frac{1}{2}$, and $M = \frac{1}{2} \rightarrow \frac{3}{2}$ transitions within the $S = \frac{5}{2}$ multiplet give rise to P_1 , P_2 , and P_5 , respectively. Hence, the ZFS for P_2 and P_5 should be equivalent in magnitude, but opposite in sign, in agreement with observation (see Table I). Peaks P_3 and P_4 correspond to the $M = -\frac{7}{2} \rightarrow -\frac{5}{2}$ and $M = -\frac{5}{2} \rightarrow -\frac{3}{2}$ transitions within the $S = \frac{7}{2}$ multiplet. As already noted, P_d corresponds to the transition between the $M = -\frac{5}{2}$ level of the $S = \frac{5}{2}$ multiplet and the $M = -\frac{7}{2}$ level of the $S = \frac{7}{2}$ multiplet. The observed temperature dependence (Fig. 2) is perfectly consistent with these assignments.

In the inset to Fig. 3(b), we display the field-orientation-dependence of B_d at several frequencies. Agreement between experiment (open squares) and theory (solid curves) is very good, including the opposing trends at lower and higher frequencies/fields. This behavior can be traced to the level repulsion (S -mixing) between the $S = \frac{7}{2}$, $M = -\frac{7}{2}$ level and various $S = \frac{5}{2}$ states as the field is tilted away from the symmetry direction of the Mn-[3 × 3] grid. As such, this non-linear frequency dependence of B_d represents evidence for quantum spin-state oscillations [12].

According to the above, P_d violates the $\Delta S = 0$ selection rule for EPR. However, labeling levels by S can be misleading because of strong S -mixing. In fact, S is no longer a good quantum number, though we retain the notation as a matter of convenience. In order to rigorously check the peak assignments, we performed a full simulation of the EPR spectrum. Results for 62 GHz are shown in Fig. 3(b) at two temperatures. The agreement with experiment is once again excellent. Most importantly, the calculations confirm the significant intensity of P_d . Hence, the mixing of spin multiplets is strong enough in Mn-[3 × 3] to observe P_d using state-of-the-art high-frequency EPR techniques (P_6 is not observed experimentally due to its 10 times lower calculated intensity). The wavefunctions of the two states involved in P_d are calculated as $0.9861|\frac{5}{2}, -\frac{5}{2}\rangle + 0.1625|\frac{7}{2}, -\frac{5}{2}\rangle - 0.0343|\frac{9}{2}, -\frac{5}{2}\rangle + \dots$, and $0.9922|\frac{7}{2}, -\frac{7}{2}\rangle - 0.1213|\frac{9}{2}, -\frac{7}{2}\rangle + 0.0270|\frac{11}{2}, -\frac{7}{2}\rangle + \dots$ (with an $|S, M\rangle$ notation for the basis functions). Hence, the ground state has 16% of $S = \frac{7}{2}$ admixed to it, or 2.6% in squared (intensity) units.

In the strong exchange limit ($|J| \gg |D|$), the zero-field energies within each multiplet are expected to scale with M as M^2 . However, this behavior is strongly perturbed in Mn-[3 × 3], with the $M = \pm\frac{3}{2}$ and $\pm\frac{1}{2}$ states even occurring out of sequence for the $S = \frac{7}{2}$ multiplet! A standard approach involves the use of an effective spin Hamiltonian, $\hat{H}_S = D\hat{S}_z^2 + B_4^0\hat{O}_4^0$, to describe each spin multiplet. For a $S = \frac{5}{2}$ state, deviations from the expected M^2 behavior may be captured by the B_4^0 parameter (for larger S , higher order terms such as $B_6^0\hat{O}_6^0$ may be important also). It is the S -mixing that gives rise to significant B_4^0 values (and higher order terms), as noted in previous works [4, 5, 8, 18]. The ratio $|B_4^0/D|$, therefore, serves as a measure of the degree of S -mixing. For the $S = \frac{5}{2}$ multiplet in Mn-[3 × 3] it is 6.6×10^{-4} , and for $S = \frac{7}{2}$ it is 29×10^{-4} . For comparison, we list the values of $|B_4^0/D|$ for some of the lowest lying states of several other molecular clusters, which are considered to show S -mixing: 0.2×10^{-4} for Fe_4 ($S = 5$); 0.5×10^{-4} for Mn_{12} ($S = 10$); 2×10^{-4} for Ni_4 ($S = 4$); and 5×10^{-4} for the $S = 2$ excited state of the ferric wheel CsFe_8 [1, 4, 8, 9]. Apparently, Mn-[3 × 3] shows the strongest S -mixing. In principle, exchange constants may be determined indirectly using Eq. (1) on the basis of deviations from

the expected M^2 behavior. However, this works only for the simplest systems, as recently demonstrated for a Ni_4 SMM [8]. In the present work, the exchange splitting was determined by direct spectroscopy via EPR.

It is apparent that the effects of S -mixing become more important as the separation between spin multiplets decreases. This argument can, however, be misleading. For example, the $S = 10$ ground and first excited $S = 9$ multiplets overlap in Mn_{12} , yet S -mixing is relatively weak ($|B_4^0/D| = 0.5 \times 10^{-4}$). In contrast, S -mixing is 10 times stronger in Mn-[3 × 3], in spite of the fact that the $S = \frac{5}{2}$ and $\frac{7}{2}$ states are well separated in energy (see Fig. 3). Evidently, other factors must be important too, such as the spatial symmetries of the relevant spin wavefunctions [5]. Therefore, one should be careful in judging the importance of S -mixing solely on the basis of the separation of spin levels, or indeed on the ratio of J and D . Understanding this issue is of great importance in terms of the design of future molecule-based magnets.

In summary, we present direct spectroscopic evidence for the mixing of spin wavefunctions in a Mn-[3 × 3] grid through the observation of an otherwise forbidden inter-spin-multiplet EPR transition. Detailed analysis in terms of a generic spin Hamiltonian provides tremendous insights into the combined effects of exchange and anisotropy in a prototypical molecular nanomagnet.

We acknowledge EC-RTN-QUEMOLNA, contract n° MRTN-CT-2003-504880, the Swiss National Science Foundation, and the US National Science Foundation (DMR0239481) for financial support.

-
- [1] G. Christou *et al.*, MRS Bull. **25**, 66 (2000); D. Gatteschi and R. Sessoli, Angew. Chem. Int. Ed. **42**, 268 (2003); W. Wernsdorfer and R. Sessoli, Science **284**, 133 (1999); S. Hill *et al.*, *ibid.* **302**, 7 (2003); E. del Barco, A. D. Kent, E. C. Yang and D. N. Hendrickson, Phys. Rev. Lett. **93**, 157202 (2004).
 - [2] Intramolecular dipolar interactions are not negligible, but have similar effects to the single-ion anisotropy and are captured by the \hat{S}_{iz}^2 terms. Thus, D values should be understood as including both anisotropy contributions.
 - [3] A. Bencini and D. Gatteschi, *Electron Paramagnetic Resonance of Exchange Coupled Clusters* (Springer, Berlin, 1990).
 - [4] E. Liviotti, S. Carretta, and G. Amoretti, J. Chem. Phys. **117**, 3361 (2002).
 - [5] O. Waldmann and H. U. Güdel, Phys. Rev. B **72**, 094422 (2005).
 - [6] N. V. Prokofev and P. C. E. Stamp, Phys. Rev. Lett. **80**, 5794 (1998).
 - [7] S. Carretta, E. Liviotti, N. Magnani, P. Santini and G. Amoretti, Phys. Rev. Lett. **92**, 207205 (2004).
 - [8] A. Wilson, J. Lawrence, E. C. Yang, M. Naknao, D. N. Hendrickson and S. Hill, Phys. Rev. B **74**, 140403(R) (2006).
 - [9] O. Waldmann, C. Dobe, H. Mutka, A. Furrer and H.

- U. Güdel, Phys. Rev. Lett. **95**, 057202 (2005); O. Waldmann, C. Dobe, H. U. Güdel and H. Mutka, Phys. Rev. B **74**, 054429 (2006).
- [10] O. Waldmann, S. Carretta, P. Santini, R. Koch, A. G. M. Jansen, G. Amoretti, R. Caciuffo, L. Zhao and L. K. Thompson, Phys. Rev. Lett. **92**, 096403 (2004).
- [11] S. Carretta *et al.*, Eur. Phys. J. B **36**, 169 (2003).
- [12] S. Carretta, P. Santini, G. Amoretti, T. Guidi, J. R. D. Copley, Y. Qiu, R. Caciuffo, G. Timco, R. E. P. Winpenny, Phys. Rev. Lett. **98**, 167401 (2007).
- [13] T. Guidi *et al.*, Phys. Rev. B **69**, 104432 (2004).
- [14] O. Waldmann, Phys. Rev. B **71**, 094412 (2005).
- [15] L. Zhao, C. J. Matthews, L. K. Thompson, and S. L. Heath, Chem. Commun., 265 (2000).
- [16] M. Mola, S. Hill, P. Goy, and M. Gross, Rev. Sci. Instrum. **71**, 186 (2000); S. Takahashi and S. Hill, *ibid.* **76**, 023114 (2005).
- [17] R. Boca, Coord. Chem. Rev. **248**, 757 (2004).
- [18] B. Pilawa *et al.*, Eur. Phys. J. B **33**, 321 (2003).